Soil Use and Management, December 2006, **22,** 405–413 doi: 10.1111/j.1475-2743.2006.00052.x

Identifying potential management zones in a layered soil using several sources of ancillary information

U. W. A. Vitharana[1], M. Van Meirvenne[1], L. Cockx[1] & J. Bourgeois[2]
[1]*Research Group Soil Spatial Inventory Techniques, Department of Soil Management and Soil Care, Ghent University, Coupure 653, 9000 Gent, Belgium, and* [2]*Department of Archaeology and Ancient History of Europe, Ghent University, Blandijnberg 2, 9000 Gent, Belgium*

Abstract

Variation in soil texture has a profound effect on soil management, especially in texturally complex soils such as the polder soils of Belgium. The conventional point sampling approach requires high sampling intensity to take into account such spatial variation. In this study we investigated the use of two ancillary variables for the detailed mapping of soil texture and subsequent delineation of potential management zones for site-specific management. In an 11.5 ha arable field in the polder area, the apparent electrical conductivity (EC_a) was measured with an EM38DD electromagnetic induction instrument. The geometric mean values of the EC_a measured in both vertical and horizontal orientations strongly correlated with the more heterogeneous subsoil clay content ($r = 0.83$), but the correlation was weaker with the homogenous topsoil clay content ($r = 0.40$). The gravimetric water content at wilting point ($\theta g_{(-1.5\ MPa)}$) correlated very well ($r = 0.96$) with the topsoil clay content. Thus maps of topsoil and subsoil clay contents were obtained from 63 clay analyses supplemented with $117\theta g_{(-1.5\ MPa)}$ and $4048EC_a$ measurements, respectively, using standardized ordinary cokriging. Three potential management zones were identified based on the spatial variation of both top and subsoil clay contents. The influence of subsoil textural variation on crop behaviour was illustrated by an aerial image, confirming the reliability of the results from the small number of primary samples.

Keywords: Site-specific management, polder soil, soil textural mapping, electromagnetic induction

Introduction

Site-specific management is the process of adjusting agricultural practices within fields according to the measured spatial variation. It has become an alternative to the traditional uniform management of agricultural fields, because it increases profitability of crop production and reduces undesirable environmental impacts by regulating production inputs according to local needs (Godwin *et al*., 2003). Identification of the within-field variation and division of a field into subunits called management zones are therefore decision-supporting steps in site-specific management (Sylvester-Bradley *et al*., 1999).

The Polder region of northwest East-Flanders, Belgium, extends to over 6840 ha and is dominated by Udifluvent and Fluvaquent soil subgroups (Soil Survey Staff, 1982). In this highly productive agricultural area, there is a need through site-specific management to minimize environmental damage which results from the uniform application of agrochemicals. For this area, Van Meirvenne & Hofman (1989) found, through investigating spatial variation in soil texture in 1 ha, a lithological discontinuity between 40 and 50 cm depth and greater spatial variation in the subsoil texture than in the topsoil. However, existing soil maps and regional studies do not reveal detailed within-field variation in soil texture (e.g. Van Meirvenne *et al*., 1990). Yet variation in soil texture often has a major effect on yield (Earl *et al*., 1996; Stafford *et al*., 1996).

The production of detailed digital soil texture maps requires considerable sampling and laboratory analysis. Alternatively, spatial information on an easy-to-measure ancillary variable can reduce this effort through selection of a carefully planned sampling design (Lund *et al*., 1999). Further, such ancillary information can be used to improve soil texture prediction using multivariate (geo)statistical

Correspondence: U. W. A. Vitharana. E-mail: u.vitharana@ugent.be
Received October 2005; accepted after revision June 2006

approaches. Many studies have explored the usefulness of secondary information for predicting soil texture usually based on Jenny's (1941) mechanistic model of soil development. Topographical attributes have been found to be very useful where there are distinct topographical variations (e.g. Odeh *et al*., 1995). Alternatively, Odeh & McBratney (2000) used remotely sensed data to map topsoil clay content. However, the use of remotely sensed data for textural mapping is limited because of the inability to infer subsoil textural variation. For textural mapping of polder soils Van Meirvenne & Hofman (1989) used a cost-effective measurement based on gravimetric water content at a matric potential of −1.5 MPa ($\theta g_{(-1.5\ \mathrm{MPa})}$) (conventionally known as 'wilting point'). Soil's apparent electrical conductivity (EC_a) has become one of the most reliable and frequently used measurements to characterize within-field variation for site-specific management. The EC_a is principally a function of solute concentration in salt-affected soils, but for non-saline soils the major influences are moisture and clay content (Kitchen *et al*., 1999). The main advantage of EC_a is that it can be measured at a high spatial resolution. The aim of the study was to identify and utilize ancillary information to produce detailed soil texture maps for both soil layers (clayey topsoil and sandy subsoil) in the polder area and then to delineate potential management zones.

Materials and methods

Study area

The study site was an 11.5 ha field in the polder area in northwest East-Flanders, Belgium (central coordinates: 51°16′17″N, 3°40′35″E, Figure 1). A series of marine transgressions following the last glaciation resulted in the deposits which form the parent material of these polder soils. Consequently, the topsoil varies from Holocene alluvial loam to clay sediments deposited over Pleistocene aeolian material with a predominantly sandy texture. From the 11th century onwards, dikes were constructed to reclaim and protect this region against new marine invasions before the land was reclaimed for agriculture by artificial drainage.

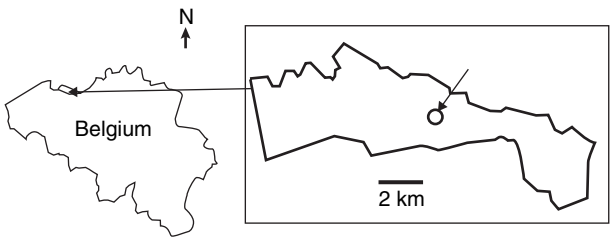

Figure 1 The polder area of northwest East-Flanders in Belgium (left) and the location of the study site within this area (right).

The soils are Aquic Udifluvents (Soil Survey Staff, 1982). The site is nearly flat with an elevation ranging from 3.2 to 3.8 m above m.s.l. The national soil map (scale 1:20 000) shows one dominant soil series: sEdp, indicating a clayey topsoil texture (E) with a shallow sandy substrate (s) and a moderately wet soil (d) with little profile development (p). A typical crop rotation is potato (*Solanum tuberosum* L.), sugar beet (*Beta vulgaris* L.) and winter wheat (*Triticum aestivum* L.).

Apparent electrical conductivity mapping and soil analysis

The apparent soil electrical conductivity (EC_a) of the field was measured on 17 November 2003 with the dual dipole electromagnetic sensor EM38DD (Geonics Limited, Canada). As recommended by Waine (1999) and Godwin & Miller (2003), the measurements were taken when the soil moisture content was close to field capacity. The EM38DD operates simultaneously in both vertical and horizontal dipole modes providing EC_a-H and EC_a-V measurements (mS m^{-1}) which are sensitive to surface and subsurface conditions (Rhoades *et al*., 1999). Our hypothesis was that topsoil and subsoil textural variation would be reflected in EC_a-H and EC_a-V measurements, respectively. The sensor connected with a GPS receiver and a field computer, was put on a non-metal sled and towed behind an all-terrain vehicle at about 15 km h^{-1} (Figure 2). Georeferenced EC_a measurements were recorded every second along lines about 5 m apart. This yielded a measurement configuration of approximately 5 m × 4 m. EC_a maps were prepared by ordinary punctual kriging following exploratory data analysis.

To investigate the relationships between EC_a and soil texture, a sampling scheme with 63 sampling points was selected based on the EC_a pattern (Figure 3b), so that spatial

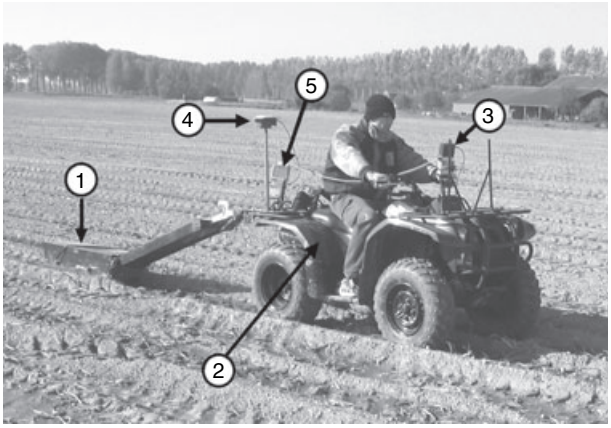

Figure 2 The mobile EC_a measuring system at the study site. 1: polyethylene sled with EM38DD; 2: all terrain vehicle; 3: GPS receiver; 4: GPS antenna; 5: field computer.

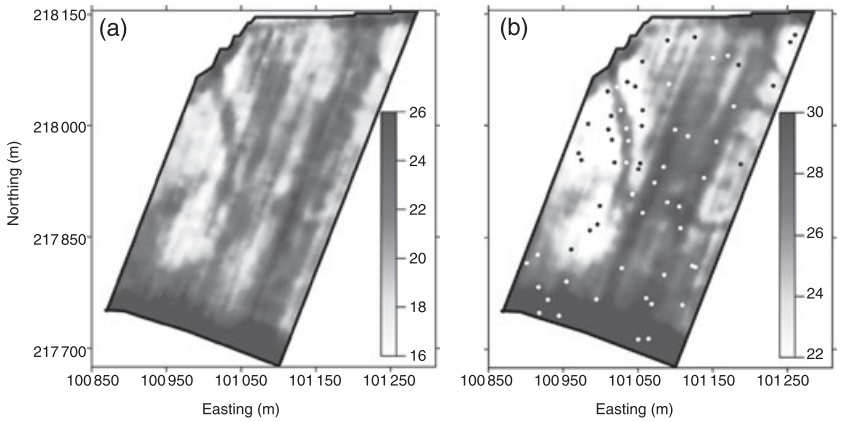

Figure 3 Interpolated values in mS m^{-1} for (a) EC_a-H and (b) EC_a-V with the 63 sampling locations shown as dots.

patterns such as the linear feature in the western part of the field were included. Sample locations were identified by GPS navigation. Topsoil (0–40 cm) and subsoil (50–80 cm) samples were taken at each sampling point, excluding any transition zone between the two layers. Three soil samples within 1 m were pooled to obtain a bulked sample. Air-dried samples were crushed and sieved through a 2-mm sieve for the soil textural analysis by the pipette method after pre-treatment for organic residues and $CaCO_3$, and the soil organic carbon content (Organic C) was determined by the conventional Walkley and Black method. The EC_a at the 63 sampling points was not measured, but co-located EC_a data for cross-variogram calculations were estimated using punctual kriging to examine the relations between EC_a and other soil properties. Kerry & Oliver (2003) showed that this as an appropriate method for obtaining co-located data by comparing different techniques.

Results and discussion

EC_a measurements

The summary statistics for EC_a are given in Table 1. The EC_a-V was larger than the simultaneously measured EC_a-H. However, high correlation ($r = 0.81$) was found between these measurements. Both EC_a-V and EC_a-H showed positively skewed data distributions with larger values observed mainly in the southern part of the field.

Despite the expected differences as a result of contrasts in soil texture between topsoil and subsoil, the EC_a-H and EC_a-V maps show very similar patterns (Figure 3). A distribution of larger and smaller EC_a values can be seen in the southern and western parts of the field. Two linear features can also be observed on the EC_a maps, one diagonally dissecting the western part having smaller EC_a values and the other extending parallel to the eastern boundary of the field with narrow side branches. Given the overall similarity between positively skewed EC_a-V and EC_a-H data, we decided to pool information from the two signals for further analysis by taking the geometric mean (GM): $EC_a\text{-GM} = (EC_a\text{-V} \times EC_a\text{-H})^{0.5}$ (Corwin & Lesch, 2005).

Soil textural variation and its relationship with EC_a-GM

Because sampling focussed on areas of greatest variation, care must be taken in using these data to describe the population. Therefore, we applied the cell declustering algorithm (Goovaerts, 1997) for all the soil properties measured at 63 sampling locations and found that neither the declustered mean nor the data distribution substantially changed for any of the soil properties. The EC_a sampling was not preferentially located in areas with higher or lower EC_a values. From the results (Table 1) it can be concluded that the topsoil was more homogeneous than the subsoil. All the subsoil properties showed markedly skewed distribution resembling the EC_a data whereas data on the topsoil properties were fairly symmetrically distributed. The CVs of the topsoil properties varied between 11 and 22.6%, compared with between 29.2 and 69.3% for the subsoil properties. The topsoil texture was mainly loam, but in the subsoil it ranged over five USDA textural classes (from sand to silt loam).

Clay content can influence other soil physical–chemical properties such as water holding capacity, hydraulic properties and cation exchange capacity, and therefore the influence of subsoil clay content on overall soil functioning cannot be neglected. The ratio between subsoil and topsoil variances was greatest for the clay fraction and thus clay content was selected as the target variable to describe variations in soil texture for both layers. There was a strong correlation ($r = 0.83$) between the EC_a-GM and subsoil clay content. However, the correlation between EC_a-GM and topsoil clay content was weak ($r = 0.40$), possibly because of the influence of the highly variable subsoil clay content on EC_a measurements.

Topsoil clay content mapping

Given the weak correlation, EC_a-GM was considered as unsuitable ancillary information for mapping topsoil clay

Table 1 Summary statistics for apparent electrical conductivity (EC_a, mS m^{-1}), topsoil gravimetric water content at a matric potential of −1.5 MPa ($\theta g_{(-1.5\ MPa)}$), top and subsoil organic C, clay, silt and sand (%)

	Number of samples	Mean	Minimum	Maximum	Variance	Skewness	CV (%)
EC_a-V	4048	26.7	18.5	46.9	20.73	1.39	17.0
EC_a-H	4048	21.4	12.2	36.4	14.09	1.02	17.6
EC_a-GM	4048	23.9	15.5	41.0	15.50	1.34	16.5
Topsoil							
Organic C	63	0.9	0.6	1.3	0.02	0.23	16.5
Clay	63	19.1	14.3	23.7	6.01	−0.03	12.9
Silt	63	36.3	20.8	54.2	67.20	0.52	22.6
Sand	63	44.6	23.4	64.8	96.84	−0.13	22.0
$\theta g_{(-1.5\ MPa)}$	117	9.4	6.6	13.8	1.05	0.37	11.0
Subsoil							
Organic C	63	0.2	0.0	0.6	0.02	0.91	56.9
Clay	63	10.2	3.2	26.5	33.49	1.14	56.6
Silt	63	20.9	3.7	60.2	209.87	1.36	69.3
Sand	63	68.9	13.6	92.9	404.93	−1.30	29.2

content and therefore the usefulness of another soil variable, $\theta g_{(-1.5\ MPa)}$ was investigated. In comparison with the soil textural analysis by the pipette method, the $\theta g_{(-1.5\ MPa)}$ measurements with pressure plate apparatus are quicker and cheaper. We found a strong linear relationship ($r = 0.96$) between topsoil clay and $\theta g_{(-1.5\ MPa)}$. Therefore, we sampled the topsoil at 54 additional locations on a 50 m × 50 m grid over the field and determined $\theta g_{(-1.5\ MPa)}$ for these samples (Table 1).

Cokriging has often been used to map a primary variable which is sparsely sampled, complemented with a secondary variable that is more densely sampled (e.g. Van Meirvenne & Hofman, 1989). In cokriging, the prediction of the primary variable depends on the spatial variation of the primary and secondary variables described by their auto-variograms and the joint spatial variation between them (coregionalization) as described by the cross-variogram. Detailed theoretical discussions on cokriging can be found elsewhere (e.g. Webster & Oliver, 2001). Two ordinary cokriging (OCK) methods were evaluated for the spatial prediction of topsoil clay content, incorporating $\theta g_{(-1.5\ MPa)}$ measurements, viz. 'traditional' and 'standardized' OCK (Goovaerts, 1997). These methods vary in the differences of the unbiasedness constraint. The traditional OCK assures the unbiasedness of the estimator by imposing two constraints (i.e. the sum of primary and secondary variable weights are 1 and 0, respectively), whereas in standardized OCK a single constraint is imposed (i.e. the sum of primary and secondary variable weights is one). Also, in standardized OCK, the estimator is modified by standardizing (rescaling) the secondary variable to the same mean as the primary variable. As a consequence, standardized OCK has the ability to overcome some of the weaknesses of traditional OCK such as the limited influence of the secondary information on the estimation. As a reference, we also used univariate ordinary kriging (OK) to predict topsoil clay content using only the 63 samples. Prediction accuracies of different techniques were evaluated by cross-validation which is a leave-one-out-in-turn procedure. The cross-validation results were interpreted using Pearson's correlation coefficient between estimated and actual values, combined with two validation indices, the mean estimation error (MEE) and the root mean-squared estimation error (RMSEE):

$$\mathrm{MEE} = \frac{1}{n}\sum_{i=1}^{n}\left(z^*(\mathbf{x}_i) - z(\mathbf{x}_i)\right)$$

$$\mathrm{RMSEE} = \sqrt{\frac{1}{n}\sum_{i=1}^{n}\left(z^*(\mathbf{x}_i) - z(\mathbf{x}_i)\right)^2}$$

where $z(\mathbf{x}_i)$ is the measured clay content, $z^*(\mathbf{x}_i)$ the estimated clay content and n the number of validated observations. The MEE and RMSEE values, being measurements of the biasedness and average error of the prediction, should approach zero as the predictions become optimal.

We used an iterative procedure to fit a linear model of coregionalization for a variogram model under the constraint of positive semi-definiteness of coregionalization matrices (Goovaerts, 1997). Figure 4 shows the omnidirectional experimental auto- and cross-variograms with fitted models:

$$\gamma_{\mathrm{topclay}}(h) = 0.99g_0 + 6.11\mathrm{Sph}(h/127.6\mathrm{m})$$

$$\gamma_{\theta g(-1.5\,\mathrm{MPa})}(h) = 0.30g_0 + 0.79\mathrm{Sph}(h/127.6\mathrm{m})$$

$$\gamma_{\mathrm{topclay}-\theta g(-1.5\,\mathrm{MPa})}(h) = 0.44g_0 + 2.07\mathrm{Sph}(h/127.6\mathrm{m})$$

where g_0 is the nugget variance, and $\mathrm{Sph}(h/a)$ the spherical model of range a (Webster & Oliver, 2001). We determined the 'hull of perfect correlation' to asses the degree of coregionalization (Webster & Oliver, 2001). This is formed from the lines of perfect positive and negative correlation. The fitted

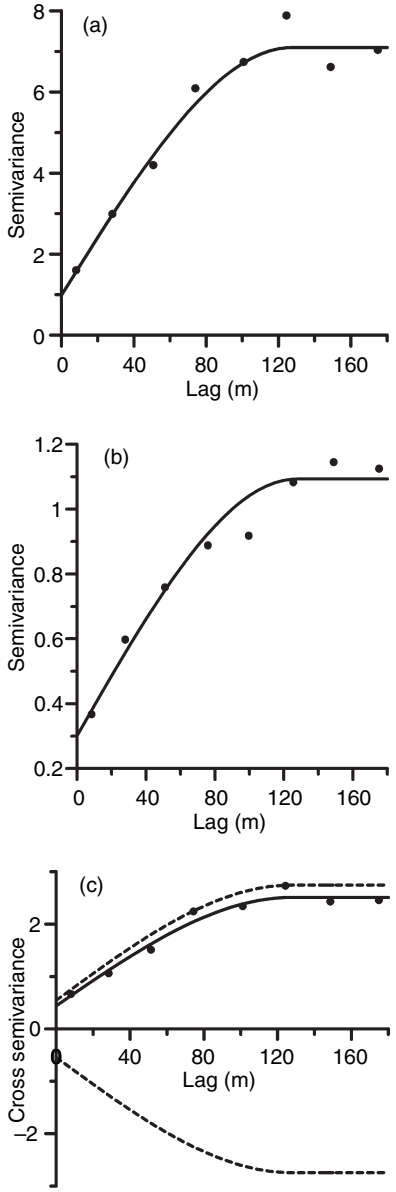

Figure 4 Experimental auto-variograms of (a) topsoil clay, (b) $\theta g_{(-1.5\ MPa)}$ and (c) cross-variogram with the fitted linear model of coregionalization. The dashed lines on the cross-variogram represent the hull of perfect positive and negative correlation.

cross-variogram model lies within and very close to this hull (Figure 4c), indicating strong coregionalization between topsoil clay and $\theta g_{(-1.5\ MPa)}$.

The cross-validation results for topsoil clay prediction by the three kriging methods are given in Table 2. The *r* and RMSEE values indicate that the incorporation of secondary information for topsoil clay mapping has slightly improved the prediction accuracy. In comparison with the OK, the standardized OCK improved the RMSEE by 4.3% whereas the improvement of traditional OCK was 3.8%. However, the relative improvement is small, possibly because of the limited

Table 2 Cross-validation indices between predicted and actual values of topsoil and subsoil clay

	Topsoil			Subsoil		
	MEE	RMSEE	*r*	MEE	RMSEE	*r*
OK	0.0002	1.86	0.60	−0.004	3.73	0.77
Traditional OCK	0.485	1.79	0.71	0.148	3.58	0.79
Standardized OCK	0.414	1.78	0.71	−0.030	3.26	0.81

OK, ordinary kriging; OCK, ordinary cokriging. MEE, mean estimation error; RMSEE, root mean-squared estimation error and *r*, Pearson's correlation coefficient.

number of additional samples of $\theta g_{(-1.5\ MPa)}$. The three methods showed MEE values close to zero justifying the unbiasedness common to geostatistical interpolation techniques.

Figure 5a shows the topsoil clay content map constructed using standardized OCK based on 63 clay contents supplemented with $\theta g_{(-1.5\ MPa)}$ measurements. This map illustrates the homogeneity of topsoil texture as revealed in the exploratory data analysis. The topsoil clay content ranges from 19 to 23% over a large area of the field whereas only a small area in the northwestern part of the field contains less clay (14–19%).

Subsoil clay content mapping

The strong correlation between subsoil clay and EC_a-GM allowed the latter to be considered as ancillary information for subsoil clay mapping. We used the same cokriging methods as in topsoil clay mapping. The experimental auto- and cross-variograms fitted with the linear model of coregionalization are shown in Figure 6:

$$\gamma_{\text{subclay}}(h) = 1.02g_0 + 24.05\text{Sph}(h/143.10\text{m})$$

$$\gamma_{\text{EC}_a\text{–GM}}(h) = 1.38g_0 + 11.09\text{Sph}(h/143.10\text{m})$$

$$\gamma_{\text{subsoilclay}-\text{EC}_a-\text{GM}}(h) = -1.14g_0 + 15.39\text{Sph}(h/143.10\text{m})$$

where g_0 is the nugget variance, and $\text{Sph}(h/a)$ the spherical model of range *a*. The auto-variograms with fitted models clearly reflect the similar spatial continuity of subsoil clay content and EC_a-GM. Strong coregionalization between subsoil clay and EC_a-GM is also evident from the fitted cross-variogram model that is close to the perfect correlation (Figure 6c).

Cross-validation of subsoil clay prediction by the three methods (Table 2) showed that standardized OCK produced the most accurate predictions with the smallest RMSEE value and the largest *r*. In comparison with the OK, the standardized OCK improved the RMSEE by 12.6%, whereas the improvement of traditional OCK was 4.0%. The relative improvement in prediction accuracy by

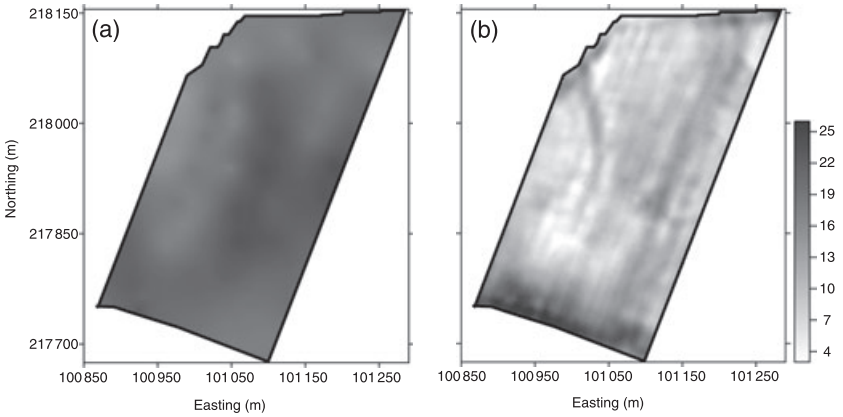

Figure 5 Predicted clay contents in percentages by standardized ordinary cokriging for (a) topsoil (b) subsoil (maps are shown with the same legend to facilitate the comparison).

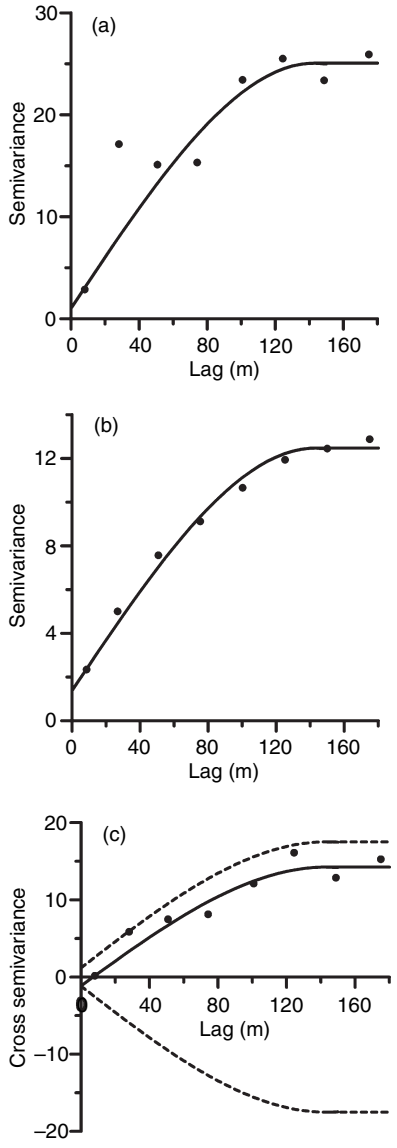

Figure 6 Experimental auto-variograms of (a) subsoil clay, (b) EC_a-GM and (c) cross-variogram with the fitted linear model of coregionalization. The dashed lines of the cross-variogram represent the hull of perfect positive and negative correlation.

standardized OCK is larger than in topsoil, possibly because of the large number of observations of EC_a. Clearly, the assignment of more weight to the secondary information is an advantage, especially when dense secondary information is available. All the methods produced unbiased subsoil clay estimates as had the topsoil clay mapping. Figure 5b shows the subsoil clay content map (standardized OCK) based on 63 texture analyses supplemented with 4048 EC_a-GM measurements. In contrast to the topsoil clay distribution a distinctive pattern of spatial variation in clay content is evident in the subsoil clay map and it resembles the EC_a map. The western and northern parts of the field contain little subsoil clay ranging from about 4 to 8%. A strip at the southern part of the field contains clayey subsoil (16–26%). The other parts of the field and especially the linear features identified on the EC_a map contain intermediate levels of subsoil clay ranging from 8 to 16%.

Delineation of potential management zones

The information on the spatial variation of topsoil and subsoil clay can be used to support site-specific management by identifying classes showing clear clay content differences. We used the fuzzy *k*-means (FKM) unsupervised classification scheme (Bezdek, 1981) to identify classes showing differences in topsoil and subsoil clay. The fuzzy classification provides a continuous grouping of objects by assigning partial class membership values, which is often preferred for the grouping of properties in the soil continuum (Odeh *et al.*, 1992). The FKM algorithm determines the membership values for objects on the basis of minimizing the objective function $J(\mathbf{M},\mathbf{C})$. Consider a set of n objects ($i = 1,\ldots,n$) each having P-attributes ($v = 1,\ldots,P$) grouped into k-classes ($c = 1,\ldots,k$), $J(\mathbf{M},\mathbf{C})$ can be expressed as:

$$J(\mathbf{M},\mathbf{C}) = \sum_{i=1}^{n}\sum_{c=1}^{k} m_{ic}^{\varphi} d_{ic}^{2}(x_i, c_c)$$

where $\mathbf{M} = m_{ic}$ is the $n \times k$ matrix of membership values, $\mathbf{C} = c_{cv}$ the $k \times P$ matrix of class centroids, c_{cv} the centroid

of class c for variable v, $c_c = (c_{c1},\ldots,c_{cp})^T$ the vector representing the centroid of class c, $x_i = (x_{i1},\ldots,x_{ip})^T$ the vector representing object i, $d^2_{ic}(x_i,c_c)$ the square distance between x_i and c_c according to a chosen distance metric (Euclidean, Mahalonobis' or Diagonal) and φ the fuzziness exponent which determines the degree of fuzziness of the classification. The fuzziness exponent ranges between one and infinity, representing crisp and completely fuzzy classifications. The predicted topsoil and subsoil clay contents at each grid cell (6.25 m^2) were used as input variables for FKM classification. We selected a fuzziness exponent value of 1.35, which was found to be appropriate for soil textural data (Odeh *et al.*, 1992). The Euclidean distance that gives equal weight to all measured variables (Bezdek, 1981) was chosen as the metric distance to enhance the influence of the highly variable subsoil clay content on the overall classification. The classification was performed using FuzME software (Minasny & McBratney, 2002) for a range of classes between two and eight. The optimum number of classes was identified on the basis of minimizing two cluster validity functions provided by FuzME: the fuzziness performance index (FPI) and the normalized classification entropy (NCE) (Roubens, 1982).

$$\mathrm{FPI} = 1 - \frac{kF - 1}{k - 1}$$

where F is the partition coefficient:

$$F = \frac{1}{n}\sum_{i=1}^{n}\sum_{c=1}^{k}(m_{ic})^2$$

$$\mathrm{NCE} = \frac{H}{\log k}$$

where H is the entropy function:

$$H = -\frac{1}{n}\sum_{i=1}^{n}\sum_{c=1}^{k} m_{ic}\log(m_{ic})$$

The FPI (constrained in the range $0 \le \mathrm{FPI} \le 1$) is a measure of the degree of membership sharing among classes, where a higher value indicates stronger sharing of membership and 0 shows distinct classes with less membership sharing. The NCE (constrained in the range $0 \le \mathrm{NCE} \le 1$) estimates the degree of disorganization in the classification with higher values indicating strong disorganization and 0 reflecting superior organization. We identified three classes (Figure 7a) as optimal for the topsoil and subsoil variation where FPI and NCE values minimized at 0.071 and 0.081, respectively. The class centroids of the three classes had very similar topsoil clay contents (class 1: 18.4%, class 2: 20.5% and class 3: 19.6%). However, the subsoil clay contents varied more: class 1 (6.8%), class 2 (11.0%) and class 3 (20.1%). The classes produced by the fuzzy k-means classification contained isolated small zones which are of no practical management value. Therefore, the fuzzy classes map was processed to obtain generalized potential management zones which are larger and sufficient to allow site-specific management. First, an image filtering technique was applied to the classified image to smooth the classes. We used a moving window (7×7 cells) to replace the value of a cell (i.e. the centre point of the moving window) based on the mode of the class values within the moving window. Then the remaining small isolated clusters were merged with the surrounding class (Figure 7b).

Water and nutrient management can be considered as key crop management practices to be modified on the basis of the delineated management zones to obtain the benefits of site-specific management. Management strategies can only be defined after further investigation of the influence of subsoil texture on overall soil quality. However, the influence of variation in soil properties on crop behaviour can be qualitatively illustrated by an aerial photograph (Figure 8) which shows the sugar beet crop in July 1989.

The image closely resembles the spatial patterns observed on the EC_a maps, particularly the EC_a-V map (Figure 3b). The vegetation in the sandy subsoil zone (class 1 of Figure 7a) appears in light grey whereas in the clayey subsoil area (classes 2 and 3 of Figure 7a) it is darker. These

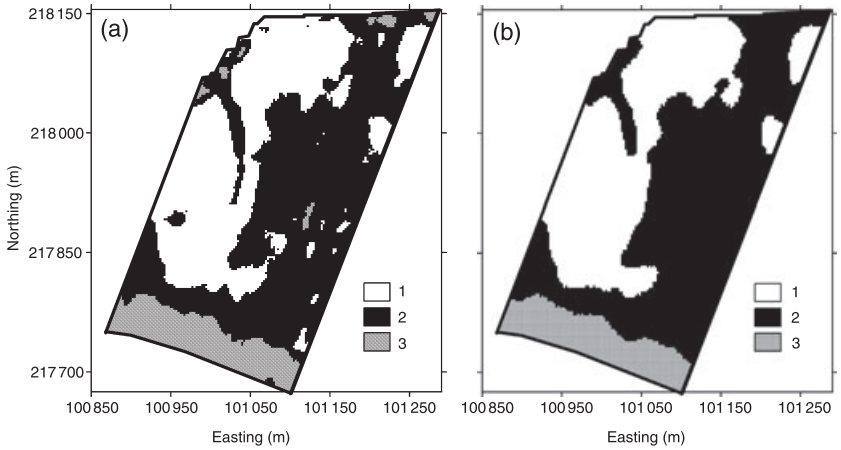

Figure 7 (a) Classes (1–3) obtained with Fuzzy k-means classification of top and subsoil clay contents and (b) generalized potential management zones.

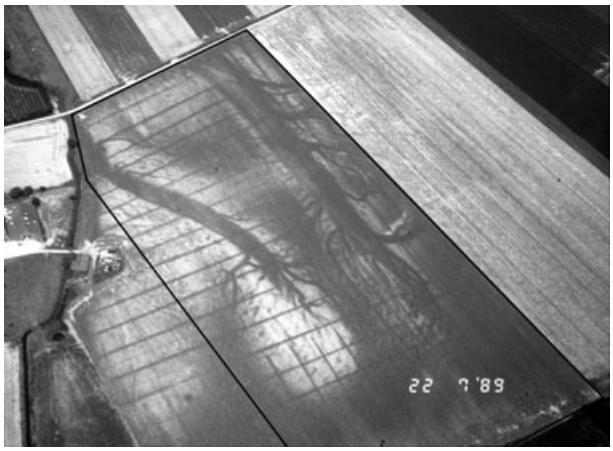

Figure 8 Oblique aerial image of the study field in July 1989 (© Department of Archaeology and Ancient History of Europe, Ghent University, Belgium, Photo: J. Semey).

differences in vegetation clearly reflect the influence of subsoil texture on crop behaviour. Specifically, the linear features identified on EC_a maps (Figure 3a,b) are apparent. Most likely these linear features represent former water channels through which marine transgressions occurred and which were subsequently filled with clayey material as shown in the map of subsoil clay content (Figure 5b). The narrow linear features in the image represent the former drainage ditch network constructed at the time of land reclamation. This strengthens the utility of aerial images as an ancillary information source to resolve spatial variation. However, in practice, obtaining geometrically accurate aerial images involves huge costs. In contrast, obtaining an EC_a inventory as ancillary information for textural mapping is more practicable and less dependent on weather or crop conditions.

Conclusions

We identified structured soil textural variation in the polder soils of northwest East-Flanders which had been inadequately identified before. The highly heterogeneous subsoil texture can cause substantial variation in crop performance and therefore, it is an important soil information for assisting site-specific management. Furthermore, electromagnetically sensed EC_a is a promising and cost-effective source of ancillary information for detailed mapping of heterogeneous subsoil. This study provides further support for the view that 'the average soil variability within the small fields of Flanders is structured enough to allow precision agriculture' (Van Meirvenne, 2003, p. 200).

Acknowledgment

We acknowledge Mr E. Van Der Schueren for granting access to his field to carry out this study. Udayakantha W.A. Vitharana thanks the University of Ghent for providing financial support under the special research fund to continue this study as a part of his PhD program. Pierre Goovaerts is thanked for the fitting of a linear model of coregionalization to our data. Further, we would like to extend our gratitude to the two anonymous referees for very helpful comments.

References

Bezdek, J.C. 1981. *Pattern recognition with fuzzy objective function algorithms*. Plenum Press, New York.

Corwin, D.L. & Lesch, S.M. 2005. Apparent soil electrical conductivity measurements in agriculture. *Computers and Electronics in Agriculture*, **46,** 11–43.

Earl, R., Wheeler, P.N., Blackmore, B.S. & Godwin, R.J. 1996. Precision farming: the management variability. *Landwards*, **51,** 18–23.

Godwin, R.J. & Miller, P.C.H. 2003. A review of the technologies for mapping within-field variability. *Biosystems Engineering*, **84,** 393–407.

Godwin, R.J., Wood, G.A., Taylor, J.C., Knight, S.M. & Welsh, J.P. 2003. Precision farming of cereal crops: a review of a six year experiment to develop management guidelines. *Biosystems Engineering*, **84,** 375–391.

Goovaerts, P. 1997. *Geostatistics for natural resource evaluation*. Oxford University Press, New York.

Jenny, H. 1941. *Factors of soil formation: a system of quantitative pedology*. McGraw-Hill, New York.

Kerry, R. & Oliver, M.A. 2003. Co-kriging when the soil and ancillary data are not co-located. In: *Precision Agriculture '03, Proceedings of the Fourth European Conference on Precision Agriculture, Berlin, 15–19 June* (eds J.V. Stafford & A. Werner), pp. 303–308. Wageningen Academic Publishers, Wageningen.

Kitchen, N.R., Sudduth, K.A. & Drummond, S.T. 1999. Soil electrical conductivity as a crop productivity measure for claypan soils. *Journal of Production Agriculture*, **12,** 607–617.

Lund, E.D., Christy, C.D. & Drummond, P.E. 1999. Practical applications of soil electrical conductivity mapping. In: *Precision Agriculture '99 Proceedings of the Second European Conference on Precision Agriculture, Odense, 11–15 July* (ed. J.V. Stafford), pp. 771–779. Sheffield Academic Press, Sheffield.

Minasny, B. & McBratney, A.B. 2002. *FuzME* Version 3. Australian Centre for Precision Agriculture The University of Sydney NSW 2006, Australia. Available at: http://www.usyd.edu.au/su/agric/acpa/fkme/program.html; accessed 17/7/2005.

Odeh, I.O.A. & McBratney, A.B. 2000. Using AVHRR images for spatial prediction of clay content in the lower Namoi Valley of Eastern Australia. *Geoderma*, **97,** 237–254.

Odeh, I.O.A., McBratney, A.B. & Chittleborough, D.J. 1992. Soil pattern recognition with fuzzy-c-means: application to classification and soil-landform interrelationships. *Soil Science Society of America Journal*, **56,** 505–516.

Odeh, I.O.A., McBratney, A.B. & Chittleborough, D.J. 1995. Further results on prediction of soil properties from terrain attributes: heterotopic cokriging and regression-kriging. *Geoderma*, **67,** 215–226.

Rhoades, J.D., Chanduvi, F. & Lesch, S.M. 1999. *Soil salinity assessment: methods and interpretation of electrical conductivity*

measurements. FAO report 57, FAO, Rome. Available at: ftp://ftp.FAO.org/agl/aglw/docs/idp57.pdf; accessed 19/8/2005.

Roubens, M. 1982. Fuzzy clustering algorithms and their cluster validity. *European Journal of Operational Research*, **10,** 294–301.

Soil Survey Staff. 1982. *Soil taxonomy*. *Agricultural handbook 436 (with amendments)*. Soil Conservation Service, USDA, Washington, DC.

Stafford, J.V., Ambler, B., Lark, R.M. & Catt, J. 1996. Mapping and interpreting yield variation in cereal crops. *Computers and Electronics in Agriculture*, **14,** 101–119.

Sylvester-Bradley, R., Lord, E., Sparkes, D.L., Scott, R.K., Wiltshire, J.J.J. & Orson, J. 1999. An analysis of the potential of precision farming in Northern Europe. *Soil Use and Management*, **15,** 1–8.

Van Meirvenne, M. 2003. Is the soil variability within the small fields of Flanders structured enough to allow precision agriculture? *Precision Agriculture*, **4,** 193–201.

Van Meirvenne, M. & Hofman, G. 1989. Spatial variability of soil texture in a polder area. II. Cokriging. *Pedologie*, **39,** 209–226.

Van Meirvenne, M., Hofman, G., Van Hove, J. & Van Ruymbeke, M. 1990. A continuous spatial characterization of textural fractions and $CaCO_3$ content of the topsoil of the polder region of NorthWest East-Flanders, Belgium. *Soil Science*, **150,** 710–716.

Waine, T.W. 1999. *Non invasive soil property measurement for precision farming*. EngD Thesis Cranfield University, Cranfield.

Webster, R. & Oliver, M.A. 2001. *Geostatistics for environmental scientists*. J. Wiley and Sons, Chichester.